Time-correlated single-photon counting with superconducting single-photon detectors

Martin J. Stevens*, Robert H. Hadfield, Robert E. Schwall, Sae Woo Nam, and Richard P. Mirin
National Institute of Standards and Technology, 325 Broadway, Boulder, CO 80305

ABSTRACT

We report use of a niobium nitride superconducting single-photon detector in a time-correlated single-photon counting experiment. The detector has a timing jitter of 68 ± 3 ps full width at half maximum with a Gaussian temporal profile. The detector's dark count rate and detection efficiency can be tuned by adjusting the bias current applied to the device. Typical values include a detection efficiency of ~1-2% and a dark count rate below 100 Hz. We use this detector to measure time-resolved photoluminescence at wavelengths up to 1650 nm, well beyond the range of conventional silicon detectors. We also use this superconducting detector to measure the emission of a quantum dot single-photon source.

Keywords: Time-correlated single-photon counting, superconducting photodetectors

1. INTRODUCTION

Time-correlated single-photon counting (TCSPC) is a highly sensitive technique that is widely used for time-resolved emission studies.[1] Typical detectors for TCSPC are avalanche photodiodes (APDs) or photomultiplier tubes (PMTs). For visible wavelengths, the fastest silicon APDs and microchannel plate PMTs offer temporal instrument response functions (IRFs) at or approaching 20 ps full width at half maximum (FWHM);[1] however, the narrow central peaks in these IRFs are typically followed by long exponential tails.[2-3] Moreover, the scarcity of good detectors suitable for wavelengths beyond ~1000 nm presents a serious limitation to TCSPC. InGaAs and Ge APDs are sensitive up to ~1600 nm, but these detectors suffer from afterpulsing problems and high dark count rates, limiting the available dynamic range.[4-7]

Recent advances in superconducting single-photon detectors (SSPDs) based on nanopatterned niobium nitride wires demonstrate their ability to overcome some of the shortcomings of conventional detectors.[8-17] SSPDs boast timing jitter as low as 18 ps FWHM, low dark count rates, and sensitivity well into the infrared. Here, we discuss the use of an SSPD in a TCSPC scheme. The device's instrument response function, which is a measure of its timing jitter, has a FWHM of 68 ± 3 ps. More importantly, the IRF has a Gaussian profile, offering a dramatic advantage over conventional detectors. The low dark count rate on this detector (< 100 Hz) allows time-resolved photoluminescence measurements with nearly five decades of dynamic range. Furthermore, we use the SSPD for measurements at wavelengths as long as 1650 nm, well outside the range of conventional silicon detectors. Finally, we show that the SSPD is sensitive enough to measure the spontaneous emission lifetime of a quantum dot single-photon source.

2. TIME-CORRELATED SINGLE-PHOTON COUNTING

Figure 1 shows a schematic of the TCSPC experiment. A semiconductor sample is optically pumped with a Ti:Sapphire laser that produces ~1 ps pulses with a center wavelength of 780 nm at an 82 MHz repetition rate. Photoluminescence (PL) from the sample is collected with an objective lens, spectrally filtered by a monochromator, and coupled into a single-mode fiber for transmission to the SSPD inside the cryocooler. Alternatively, the monochromator output can be diverted to a Si APD by inserting a mirror before the fiber coupler (not shown).

*marty@boulder.nist.gov; phone 1 303 497-4740; fax 1 303 497-3387

Advanced Photon Counting Techniques, edited by Wolfgang Becker, Proc. of SPIE
Vol. 6372, 63720U, (2006) · 0277-786X/06/$15 · doi: 10.1117/12.685447

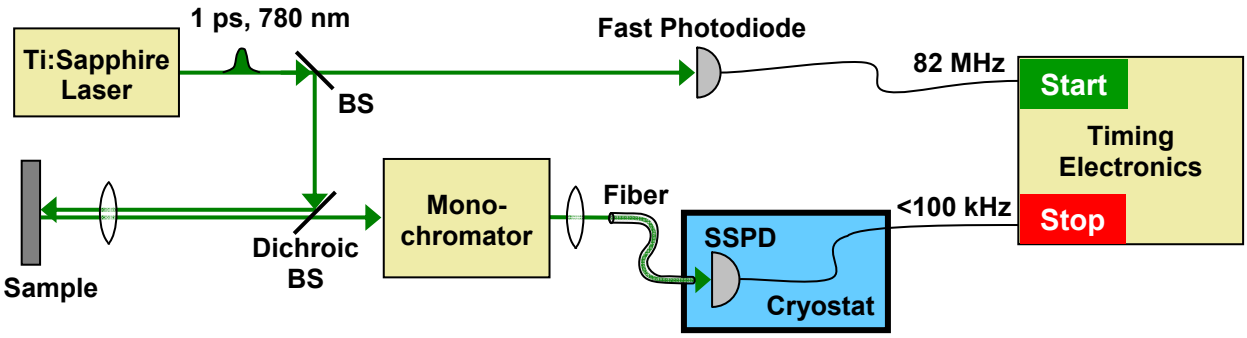

Fig. 1. TCSPC experimental geometry, where BS is a beamsplitter.

The heart of TCSPC is the timing electronics. The fast photodiode delivers a clock signal—at the laser repetition rate of 82 MHz—to the timer's start. The voltage pulse from the single-photon detector—either the SSPD or an APD—stops the timer. The electronics contribute a timing jitter of less than 30 ps to the measurements; this adds in quadrature with any jitter from the detector and the optical components.[1] In the timing electronics, the start and stop inputs to the electronics each pass through a constant fraction discriminator before engaging a digital time-to-amplitude converter (TAC). The TAC output is fed into a multichannel analyzer, which builds up a histogram of counts versus start-stop time interval (τ). The start rate is kept less than ~100 kHz to ensure an average of less than about one count per 1000 excitation pulses, preventing a pile-up of counts in the early time bins. Under these conditions, the resulting histogram is proportional to the time-resolved PL intensity, giving a direct measure of the sample's spontaneous emission lifetime.[1]

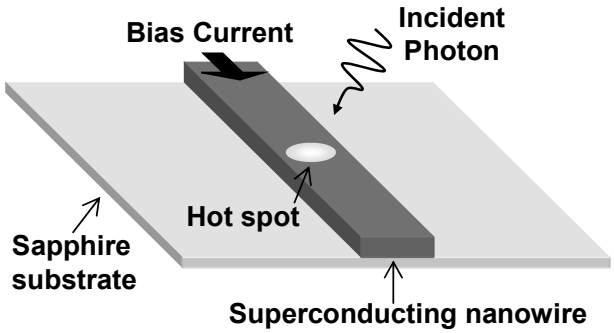

Fig. 2. Principle of operation of a superconducting single-photon detector. An absorbed photon creates a resistive hot spot in the wire, resulting in an output voltage pulse.

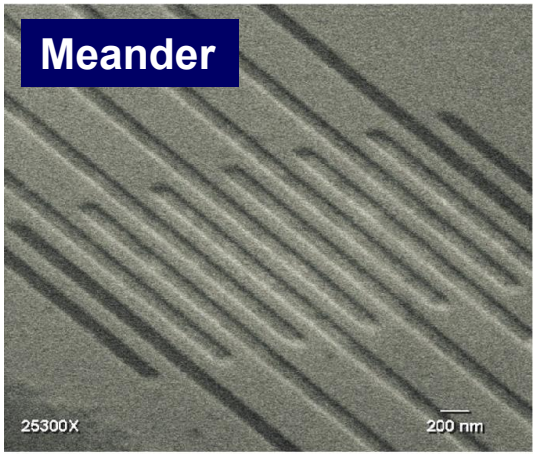

Fig. 3. Scanning electron microscope image of an SSPD meander device similar to the one discussed in the text.

3. SUPERCONDUCTING SINGLE-PHOTON DETECTOR

The SSPD device is a narrow, superconducting niobium nitride (NbN) wire embedded in a 50 Ω transmission line. The superconducting track is current biased just below its critical current I_C. When this wire absorbs a photon, it momentarily creates a nonsuperconducting hot spot, as shown in Fig. 2. As a result, a small voltage is developed briefly across this resistive section of the track, causing a high-speed voltage pulse to propagate along the transmission line.[12-15] The early devices, consisting of a single straight NbN wire, suffered from low detection efficiency,[8] owing to the difficulty of coupling light to such a small detector area. The SSPDs used here boost detection efficiency through a 100 nm width meander line (see Fig. 3) with 200 nm pitch, covering a 10 μm × 10 μm area.[9]

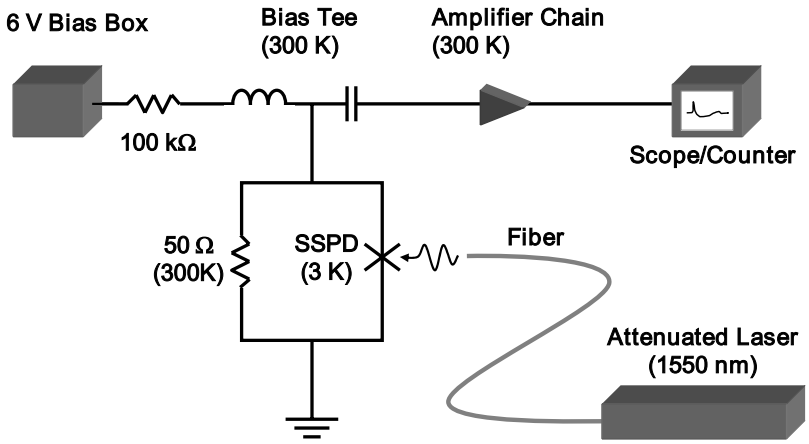

Fig. 4. Schematic of bias and readout circuit.

Since the superconducting detector must be operated at temperatures near 4 K, we have packaged the device in a practical, cryogen-free system using a commercially available cryocooler.[15] In this system, a low-noise current source is used to bias the detector, and commercial, room-temperature rf amplifiers with adequate bandwidth and sufficiently low noise figure amplify the pulses generated by the detector, as shown in Fig. 4. A typical amplified voltage pulse is plotted in Fig. 5. The amplified pulses are fed directly into the stop input of the timing electronics. For the bias conditions used here, the SSPD exhibits no measurable afterpulsing.

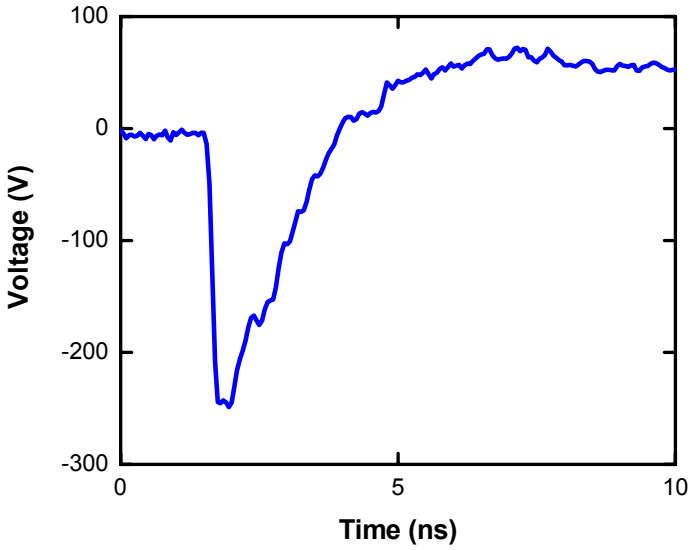

Fig. 5. Voltage pulse from an SSPD.

Light is coupled to the detector by a method previously developed at NIST for transition edge sensor single-photon detectors,[18,19] as shown in Figs. 6-7. Each detector is mounted on a small metal block. Aluminum wirebonds connect the on-chip coplanar waveguide to an SMA connector. High-speed coaxial cables that are heatsunk at 2.9 K and 40 K conduct the signal from the detector to room temperature. A polished single-mode optical fiber is held in a second metal block positioned over the chip carrier. The fiber in the ferrule holder is aligned over the detector by viewing the transmission of fiber-coupled 1550 nm light through the chip with an infrared microscope. The position of the fiber/fiber holder is adjusted such that the detector blocks the light. This method allows alignment of the fiber to the chip with a precision of a few micrometers. The optical fiber enters the cryostat via an epoxy feedthrough.

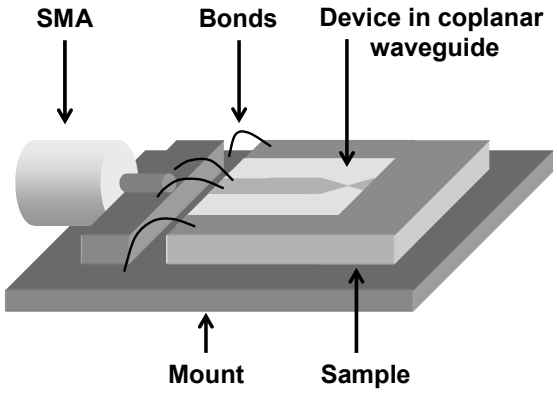

Fig. 6. Sample mount.

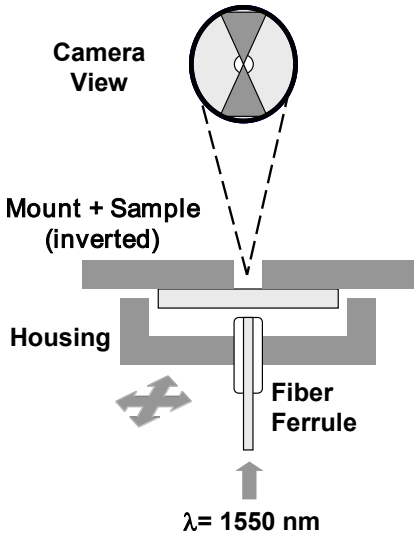

Fig. 7. Drawing of fiber alignment procedure.

Stable operation (constant detection efficiency and dark count rate) of the SSPD requires stable operating temperatures.[8-11] For the SSPD system, we use a compact, closed-cycle, cryogen-free, Gifford-McMahon-type cryocooler.[20] The refrigerator has sufficient capacity to cool a number of detectors simultaneously to 2.9 K. However, the cold head temperature fluctuates approximately ±0.3 K peak-to-peak at 1.2 Hz. To mitigate these fluctuations, we passively temperature stabilize the detector assembly by weakly coupling the detector stage to the cold stage; this reduces the fluctuations to a few millikelvin.

We determine the system detection efficiency (DE) at 1550 nm using an attenuated, pulsed telecommunications laser. A conventional power meter is used to measure the average power output from the pulsed laser. Given the power, pulse repetition frequency (f = 1 MHz) and wavelength, we can estimate the mean number of photons per pulse, μ. For a

given bias current I_{Bias}, the total count rate R is recorded as a function of μ. The single-photon detection efficiency, η, coupled to a source with a Poisson photon number distribution (such as a laser), can be extracted by fitting to the relation

$$R \approx D + f\left(1 - e^{-\eta\mu}\right), \tag{1}$$

where D is the dark count rate. Figure 8 shows the results of this DE measurement procedure for three values of bias current, along with fits to Eq. (1). For a single-photon counting detector, when $\eta\mu << 1$, R should increase linearly with μ, since Eq. (1) reduces to

$$R \approx D + f\eta\mu\,. \tag{2}$$

This linear dependence on μ is evident in the excellent agreement between the data and fits in Fig. 8. By contrast, if the detector were counting multiphoton events, rather than single-photon events, then R would have a superlinear dependence on μ. Note that for I_{Bias} = 0.82 I_C (data set B), even with 0.1 photons per laser pulse, nearly 90% of the counts from the detector are signal counts. Intrinsic detection efficiencies of up to 10 % for the same type of detectors at 1550 nm have been reported.[11] For this packaged, fiber-coupled detector, the maximum observed DE at 1550 nm is ~2.7%; however, the dark count rate is quite high for this bias current (~6 kHz). Note that the SSPD used in the TCSPC measurements presented below has a lower DE than the one characterized in Fig. 8.

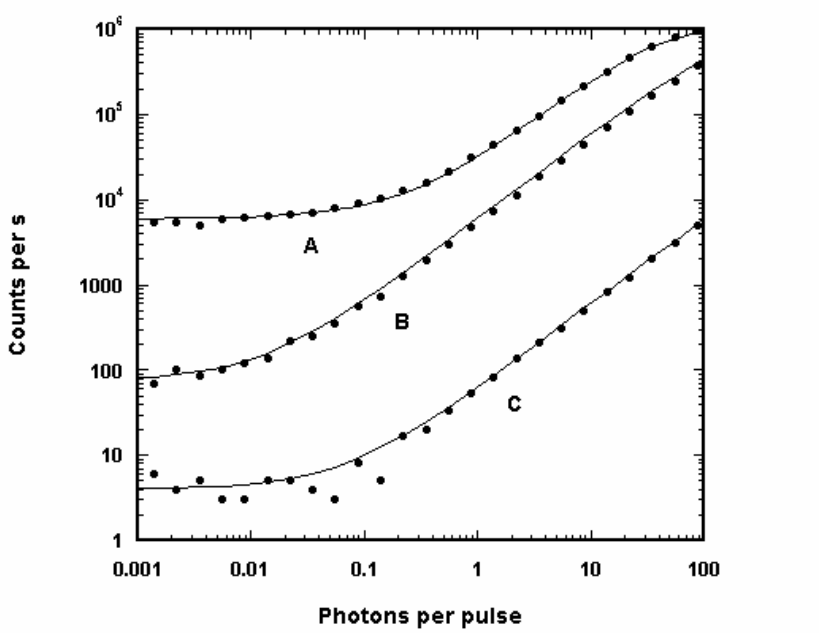

Fig. 8. Determination of efficiency and dark count rate of an SSPD. For data sets A, B, and C, I_{Bias} is set at 96%, 82%, and 65% of I_C, respectively. The solid curves are fits to Eq. (1) for dark count rate D and detection efficiency η. The fits yield values of D = 6 kHz and $\eta = 2.7\times10^{-2}$ for data set A; D = 75 Hz and $\eta = 6\times10^{-3}$ for B; and D = 4.5 Hz and $\eta = 6\times10^{-5}$ for C.

At 902 nm, we find SSPD system detection efficiency by exciting a sample that emits at this wavelength and holding the PL light level constant. We then compare the SSPD's count rate to the count rate on a Si APD with a known DE. The maximum detection efficiency of 3% and maximum dark count rate of 1 kHz are obtained for I_{Bias} near I_{C}. Below I_{C}, the dark count falls more rapidly than the detection efficiency, allowing us to achieve a 2% detection efficiency at ~100 Hz dark count rate. This device (which is not the one measured in Fig. 8) has a DE of ~1% at 1550 nm; the higher DE at 902 nm is due primarily to the higher photon energy at 902 nm.

4. RESULTS AND DISCUSSION

4.1 Instrument Response Functions

To compare the performance of the SSPD with conventional silicon APDs, we insert each detector into the TCSPC setup. First, we characterize the timing jitter by measuring each detector's temporal IRF. To measure the IRF of a detector, we tune the monochromator to 780 nm to pass only the heavily attenuated laser pulse train. Results are shown in Fig. 9. The SSPD response shown here is fit well—over nearly *five decades* of dynamic range—by a Gaussian with a FWHM of 71 ps. Averaging several measurements yields a timing jitter of 68 ± 3 ps FWHM for the entire measurement system—including all optical and electronic components. This jitter is independent of count rate between 50 Hz and 1 MHz.

Note that timing jitter as low as 18 ps has been reported for similar SSPD devices; however, those measurements were done in a regime where the detector produced a voltage pulse for *every* incident laser pulse.[10,11] Here, by contrast, we report timing jitter measurements for the much lower count rates required for TCSPC. Differences in our device, amplifier, or timing electronics may also contribute to this discrepancy with previous work. Furthermore, the IRF measured here includes time jitter from all optical and electronic components in the system.

For comparison, Fig. 9 also shows the measured IRFs of a conventional silicon APD (FWHM ≈ 400 ps) and a fast Si APD (FWHM ≈ 40 ps). Although the fast APD has a narrow main peak, it also has an exponential tail that persists for several hundred picoseconds. This diffusion tail, which is typical of APDs, is caused by the slow diffusion of photoexcited carriers from the neutral region into the high-field region of the device.[3] The relative magnitudes of the main peak and tail—and thus the shape of the total IRF—depend strongly on wavelength, further complicating the analysis of measured decay curves.[3,21]

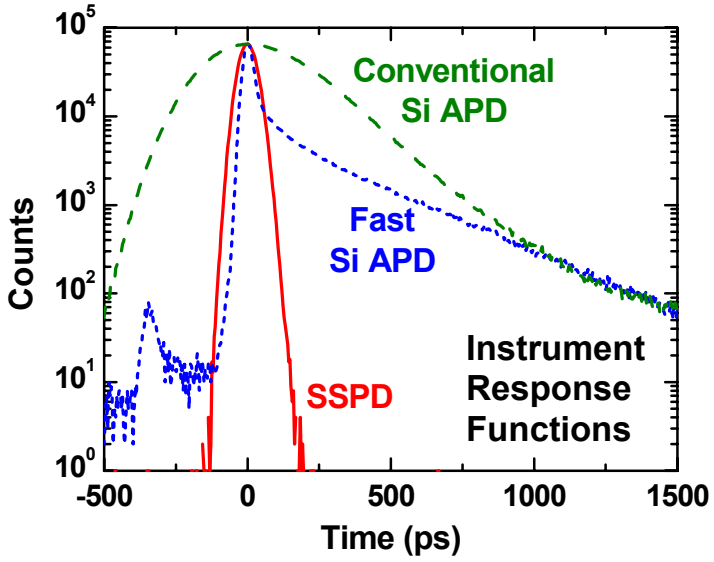

Fig. 9. Measured instrument response functions of three detectors.

Table 1 summarizes the performance of these three detectors. The Si detectors' efficiencies listed are the values given by their manufacturers. The IRF FWHM of the two Si APDs are consistent with the manufacturer specifications, assuming ~20 ps jitter contribution from our TCSPC electronics. The SSPD's response function has a FW(1/100)M (full width at one one-hundredth maximum) of ~190 ps, and a FW(1/1000)M of ~240 ps. Clearly, these widths are much narrower than the corresponding widths for either Si APD studied here. The fastest available Si APDs and microchannel plate photomultiplier tubes have IRFs between 20 and 30 ps FWHM.[1] However, these IRFs are typically plagued by long diffusion tails like those visible in Fig. 9.[3,22] Dual-junction Si APDs offer improved temporal response shapes with FW(1/100)M and FW(1/1000)M values that are similar to the SSPD studied here.[3,22] Nevertheless, since these dual-junction devices rely on silicon, they are not sensitive to wavelengths beyond 1 μm.

Table 1. Comparison of the three single-photon detectors discussed in the text.

Detector	IRF FWHM	IRF FW(1/100)M	IRF FW(1/1000)M	Efficiency @ 900 nm	Dark Counts
Conventional Si APD	400 ps	1282 ps	1948 ps	38%	~100 Hz
Fast Si APD	40 ps	787 ps	1531 ps	5%	~50 Hz
SSPD	68 ps	190 ps	236 ps	2%	< 30 Hz

4.2 Quantum well emission at 935 nm

The advantage of the SSPD over the Si detectors is evident in Fig. 10, which shows lifetime measurements of a GaAs/InGaAs quantum well (QW). This sample has an emission peak at 935 nm and was chosen for its relatively short lifetime. Only the SSPD-measured lifetime clearly shows a clean single exponential decay, even without deconvolving the IRF. Although the SSPD has a fairly low detection efficiency, its low dark count rate allows measurements with several decades of dynamic range simply by increasing the integration time—although here it is still under three minutes. In addition, identification of multi-exponential processes should be far more straightforward with the SSPD's Gaussian-shaped IRF than with the multi-component response of either Si APD.

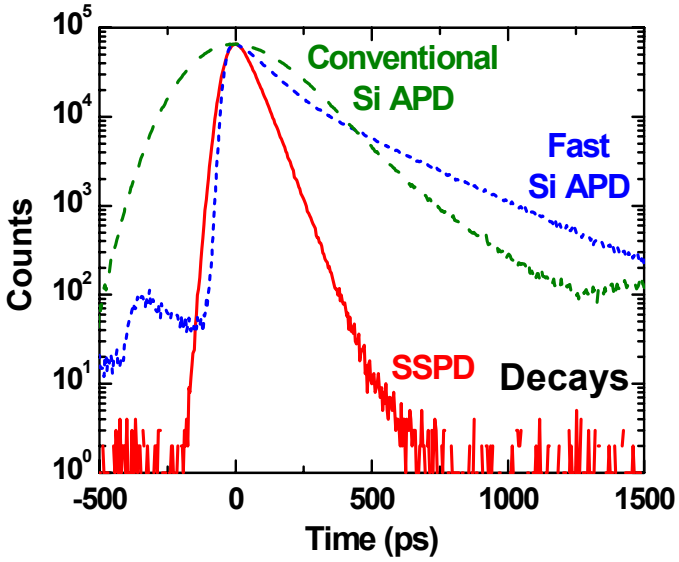

Fig. 10. GaAs/InGaAs quantum well emission at 935 nm measured with three detectors.

4.3 InGaAs epilayer emission at 1650 nm

Figure 11 shows the use of an SSPD to measure the spontaneous emission lifetime of an InGaAs epilayer that is lattice matched to InP and emits at 1650 nm. Green triangles represent the SSPD IRF, blue circles show the time-resolved PL data, and the red curve is a fit to the decay data. This fit is the measured IRF convolved with an exponential with a 290 ps decay constant. Note that the data in Fig. 11 could not have been acquired with either of the Si APDs, since this wavelength is well outside the photosensitive range of silicon.

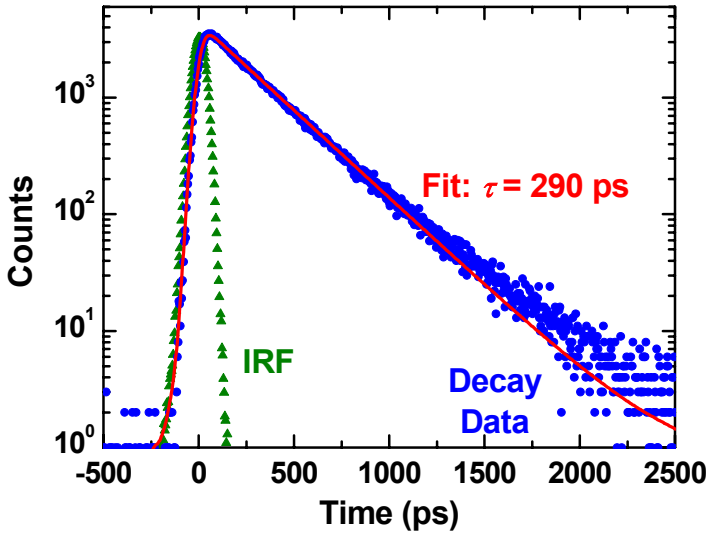

Fig. 11. Time-resolved PL measured from an InGaAs epilayer at room temperature emitting at 1650 nm.

4.4 Single quantum dot emission at 902 nm

Finally, Fig. 12 illustrates that the SSPD is sensitive enough to measure the spontaneous emission lifetime of a single quantum dot. As discussed in Ref. 15, we use a Hanbury Brown-Twiss interferometer to verify that this quantum dot emits one photon at a time. Fitting the decay data to the convolution of the IRF with a single exponential yields a decay time of ~400 ps. This fit is shown as a solid red line in Fig. 12. The rising edge in the emission itself should be dominated by the carrier capture time, which is typically under 50 ps;[23] a sufficiently fast SSPD paired with fast electronics could permit one to fully resolve this rising edge, allowing measurement of this capture time for a single dot.

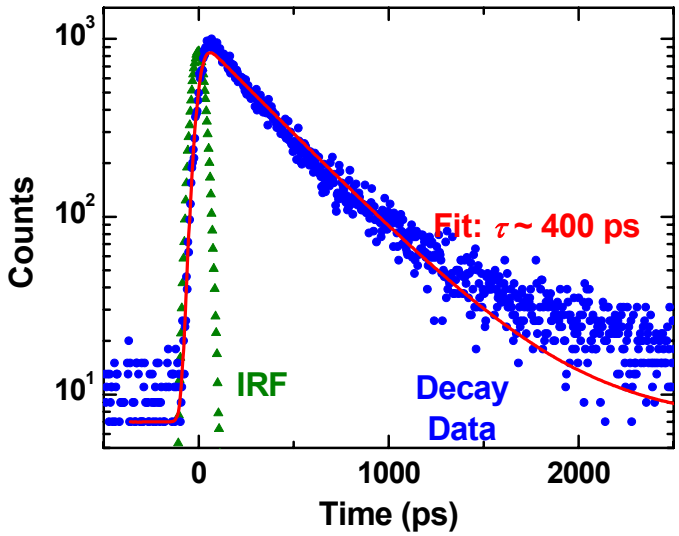

Fig. 12. Time-resolved PL measured from a single InGaAs QD at 4 K emitting at 902 nm.

5. SUMMARY

In this work, we have demonstrated the use of a superconducting single-photon detector in a time-correlated single-photon counting measurement system. Unlike conventional silicon APDs, this detector has a Gaussian temporal response function, which is clearly advantageous for determining short lifetimes and analyzing multi-exponential decays. The superconducting detector is sensitive to wavelengths longer than 1 μm, beyond the range of silicon detectors. It also

has much lower dark count rates and afterpulsing probability than either InGaAs or Ge APDs. With these advantages, superconducting detectors like the one studied here should have many practical uses, from characterizing weakly emitting materials and fiber-based quantum key distribution[24] to a host of other applications requiring high time resolution and single-photon sensitivity in the infrared region of the spectrum.

ACKNOWLEDGMENTS

We thank N. Bergren, J. Berry, C. Elliot, E. Gansen, S. Gruber, T. Harvey, A. Miller, A. Norman, K. Silverman, M. Su, and H. Yeh for contributions to this work. We thank G. Gol'tsman for providing the superconducting detectors and A. Holmes for providing the InGaAs sample discussed in Section 4.3.

REFERENCES

1. W. Becker, *Advanced Time-Correlated Single Photon Counting Techniques* (Springer Series in Chemical Physics, Vol. 81), Springer, Berlin, 2005.
2. S. Cova, A. Lacaita, M. Ghioni, G. Ripamonti, and T. A. Louis, "20-ps timing resolution with single-photon avalanche diodes," *Rev. Sci. Instr.*, vol. 60, pp. 1104-1110, Jun. 1989.
3. S. Cova, M. Ghioni, A. Lotito, I. Rech, and F. Zappa, J. Mod. Opt., **51**, 1267 (2004).
4. J. M. Smith, P. A. Hiskett, I. Gontijo, L. Purves, and G. S. Buller, Rev. Sci. Instr. **72**, 2325 (2001).
5. J. G. Rarity, T. E. Wall, K. D. Ridley, P. C. M. Owens, and P. R. Tapster, "Single-photon counting for the 1300-1600-nm range by use of Peltier-cooled and passively quenched InGaAs avalanche photodiodes," Appl. Opt., vol. 39, pp. 6746-6753, Dec. 2000.
6. J. S. Vickers, R. Ispasoiu, D. Cotton, J. Frank, B. Lee, and S. Kasapi, "Time-resolved photon counting system based on a Geiger-mode InGaAs/InP APD and a solid immersion lens," *Proc. IEEE 16th Annual Meeting Lasers and Electro-Optics Society, LEOS 2003* (Institute of Electrical and Electronics Engineers, New York) vol. 2, pp. 600-601, Oct. 2003.
7. G. Ribordy, N. Gisin, O. Guinnard, D. Stucki, M. Wegmuller, and H. Zbinden, J. Mod. Opt., **51**, 1381 (2004).
8. G. N. Gol'tsman, O. Okunev, G. Chulkova, A. Lipatov, A. Semenov, K. Smirnov, B. Voronov, A. Dzardanov, C. Williams, and R. Sobolewski, "Picosecond superconducting single-photon optical detector," *Appl. Phys. Lett.*, vol. 79, pp. 705-707, Aug. 2001.
9. A. Verevkin, J. Zhang, R. Sobolewski, A. Lipatov, O. Okunev, G. Chulkova, A. Korneev, K. Smirov, G. N. Gol'tsman, and A. Semenov, "Detection efficiency of large-active-area NbN single-photon superconducting detectors in the ultraviolet to near-infrared," *Appl. Phys. Lett.*, vol. 80, pp. 4687-4689, Jun. 2002.
10. A. Korneev, P. Kouminov, V. Matvienko, G. Chulkova, K. Smirnov, B. Voronov, G. N. Gol'tsman, M. Currie, W. Lo, K. Wilsher, J. Zhang, W. Słysz, A. Pearlman, A. Verevkin, and R. Sobolewski, Appl. Phys. Lett. **84,** 5338 (2004).
11. A. Verevkin, A. Pearlman, W. Słysz, J. Zhang, M. Currie, A. Korneev, G. Chulkova, O. Okunev, P. Kouminov, K. Smirnov, B. Voronov, G. N. Gol'tsman, and R. Sobolewski, J. Mod. Opt. **51**, 1447 (2004).
12. A. D. Semenov; G. N. Gol'tsman; A. A. Korneev, "Quantum detection by current carrying superconducting film," *Physica C*, vol. 351, pp. 349-356, Apr. 2001.
13. G. N. Gol'tsman, A. Korneev, I. Rubtsova, I. Milostnaya, G. Chulkova, O. Minaeva, K. Smirnov, B. Voronov, W. Słysz, A. Pearlman, A. Verevkin, and R. Sobolewski, phys. stat. sol. (c) **2**, 1480 (2005).
14. R. H. Hadfield, A. J. Miller, S. W. Nam, R. L. Kautz, and R. E. Schwall, "Low-frequency phase locking in high-inductance superconducting nanowires," *Appl. Phys. Lett.*, vol. 87, art. 203505, Nov. 2005.
15. R. H. Hadfield, M. J. Stevens, S. G. Gruber, A. J. Miller, R. E. Schwall, R. P. Mirin, and S. W. Nam, Opt. Exp. **13**, 10846 (2005).
16. A. J. Kerman, E. A. Dauler, W. E. Keicher, J. K. W. Yang, K. K. Berggren, G. Gol'tsman, and B. Voronov, Appl. Phys. Lett. **88**, 111116 (2006).
17. M. J. Stevens, R. H. Hadfield, R. E. Schwall, S. W. Nam, R. P. Mirin and J. A. Gupta, "Fast lifetime measurements of infrared emitters using a low-jitter superconducting single photon detector," *Appl. Phys. Lett.*, vol. 89, art. 031109, Jul. 2006.
18. D. Rosenberg, A. E. Lita, A. J. Miller, S. W. Nam, and R. E. Schwall, "Performance of photon-number resolving transition-edge sensors with integrated 1550 nm resonant cavities," IEEE Trans. Appl. Superconductivity, vol. 15, pp. 575-578, Jun. 2005.

19. D. Rosenberg, A. E. Lita, A. J. Miller, and S. W. Nam, "Noise-free high-efficiency photon-number-resolving detectors," *Phys. Rev. A*, vol. 71, art. 061803(R), Jun. 2005.
20. R. Radebaugh, "Refrigeration for Superconductors," *Proc. IEEE*, vol. 92, pp. 1719-1734, Oct. 2004.
21. R. Krahl, A. Bülter, and F. Koberling, "Performance of the Micro Photon Devices PDM 50CT SPAD detector with PicoQuant TCSPC systems," PicoQuant GmbH *TechNote MPD SPAD* (2005).
22. A. Spinelli, M. A. Ghioni, S. D. Cova, and L. M. Davis, IEEE J. Quant. Electron. **34**, 817 (1998).
23. R. Heitz, M. Veit, N. N. Ledentsov, A. Hoffmann, D. Bimberg, V. M. Ustinov, P. S. Kop'ev, and Zh. I. Alferov, "Energy relaxation by multiphonon processes in InAs/GaAs quantum dots," *Phys. Rev. B*, vol. 56, pp. 10435-10444, Oct. 1997.
24. N. Gisin, G. Ribordy, W. Tittel, and H. Zbinden, Rev. Mod. Phys. **74**, 145 (2002).